

Camera Source Identification of Digital Images Based on Sample Selection

Zhihui Wang, Hong Wang and Haojie Li

DUT-RU International School of Information & Software Engineering,
Dalian University of Technology.
Economy and Technology Development Area - China
[e-mail: lihaojieyt@gmail.com]
*Corresponding author: Haojie Li

*Received July 18, 2017; revised December 20, 2017; accepted March 22, 2018;
published July 31, 2018*

Abstract

With the advent of the Information Age, the source identification of digital images, as a part of digital image forensics, has attracted increasing attention. Therefore, an effective technique to identify the source of digital images is urgently needed at this stage. In this paper, first, we study and implement some previous work on image source identification based on sensor pattern noise, such as the Lukas method, principal component analysis method and the random subspace method. Second, to extract a purer sensor pattern noise, we propose a sample selection method to improve the random subspace method. By analyzing the image texture feature, we select a patch with less complexity to extract more reliable sensor pattern noise, which improves the accuracy of identification. Finally, experiment results reveal that the proposed sample selection method can extract a purer sensor pattern noise, which further improves the accuracy of image source identification. At the same time, this approach is less complicated than the deep learning models and is close to the most advanced performance.

Keywords: Image source identification, sensor pattern noise, random subspace method, sample selection

1. Introduction

With the development of technology, more and more devices can capture images. At the same time, image editing tools are becoming commoner and everyone can modify the images easily. This leads to a rise in digital crime rate and false advertising. So effective techniques for digital camera forensics are urgently needed to prevent malicious forgery and identify the authenticity of images. One of the important topics in digital camera forensics is camera source identification, which is used to map the image to its source device. It will help law enforcement agencies in providing legal evidences for digital crimes or protecting consumer interests by constraining merchants' false advertising. However, source camera identification is still a hard task, especially the device-level identification.

The images taken by different cameras contain some features caused by the internal hardware and software facilities, such as the camera lens, sensor pattern noise, color filter array interpolation algorithm and image multidimensional feature vector. K. S. Choi *et al.*[1] introduce the feature of radial lens distortion based on a multidimensional eigenvector to identify the source of images, using three different models of cameras, and reach an average of 91.5% identification accuracy. However, this method cannot identify different individual cameras of the same camera models and depends on straight line in images, so this method has very few follow-up studies. Commonly used cameras only obtain one type of color information from three-channel RGB when capturing pixels; the remaining two types of color information are obtained using a Color Filter Array (CFA) demosaicking interpolation algorithm; otherwise, the cost of production is expensive, and matching is difficult. Different templates are used to interpolate in different cameras. So we can identify the image source by obtaining the image interpolation rule, and this idea is called the mosaic algorithm. John S. Ho *et al.*[2] put forward a method to distinguish a complex mosaic algorithm according to the correlation between channels, adding a new feature dimension for existing correlation algorithms. The experiment results show 94.5% average identification accuracy on four different camera models. However, this method fails to identify compressed images and different individual cameras of the same model because the models use the same CFA interpolation algorithm. Q. Liu *et al.*[3] propose a new identification method based on a multidimensional feature vector, and the average identification accuracy is above 95%. However, this method cannot identify different individuals of the same model, and the data set must be large enough to ensure identification accuracy.

Sensor pattern noise (SPN) is similar to the fingerprint of a camera and plays an important role in digital camera image source identification. It has been widely used in image source identification, image classification, forgery detection, etc. J. Lukas *et al.*[4] propose a method based on image pattern noise, calculating the correlation coefficient with the query image SPN and camera reference SPN to determine whether the query image derives from a camera. This method has high recognition efficiency and can identify different individuals of the same camera model, but the image content has a large influence on the identification result. R. Li *et al.*[5] bring in principal component analysis (PCA) to this method to reduce the dimension of the feature set and the influence of the image content to a certain extent. To resolve the problem of image content influence on identification, R. Li *et al.*[6] also proposed a random subspace method (RSM) based on principal component analysis. In the present study, we combine sample selection with the random subspace method. Different areas of an image have different complexity, so before extracting SPN, we partition image into patches and analyze

their complexity. By selecting a patch with less complexity as a sample area to extract purer pattern noise, the identification performance is further optimized. Moreover, this course is part of an offline process, so it does not influence speed. The experimental results reveal that our method can obtain an SPN that is less affected by the image details and achieves higher average identification accuracy than previous methods.

The rest of this paper is organized as follows. In Section 2, we introduce some methods based on SPN that are associated with the proposed method. In Section 3, we present our sample selection method for the source identification of digital images. Experimental results are reported in Section 4, followed by the conclusion in Section 5.

2. Related Work

The method based on SPN proposed by J. Lukas [4] can be roughly divided into three steps: 1) First, extract the query SPN from the query image; 2) Second, summarize from the camera's reference SPN from a large number of images taken by this camera; 3) Last, calculate the correlation coefficient between the query and reference SPN. If the correlation coefficient is bigger than the threshold, the query image is considered to have been taken by this camera; otherwise, the query image is considered to have been taken by the other camera. This method is simple in theory, but the extracted noise contains certain scene details, and the redundant information will have great influence on image source identification. Feature selection is one important technique for dimensionality reduction that involves identifying a subset of the most useful features. Z. Li *et al.* [7] propose a novel unsupervised feature selection scheme, named clustering-guided sparse structural learning (CGSSL), which effectively selects necessary features across the entire feature space by an efficient iterative algorithm. However, CGSSL does not explicitly control the redundancy existing on the selected features, so they extend their work to nonnegative spectral analysis with constrained redundancy (NSCR) [8]. The problem of feature selection is formulated as an optimization problem with a well-defined objective function, through simple yet efficient iterative algorithm to select the most discriminative features while control the redundancy between the selected features. Z. Li *et al.* [9] propose a novel robust structured subspace learning (RSSL) algorithm by integrating image understanding and feature learning into a joint learning framework. The learned subspace reduces the semantic gap between the low-level visual features and the high-level semantics. Experimental results prove that the proposed method is effective and efficient. L. Zheng *et al.* [10] introduce PCA to eliminate the noise resulting from CFA interpolation. R. Li *et al.* [5] propose a feature extractor that can extract the principal component of SPN from original noise residual, using low change reference images (such as blue sky images) as the training sample at the same time; such a feature extractor has the best training effect on the extracted SPN principal component. Experiment results show that the optimized feature extractor is effective at restraining redundancy and the interference component.

To build a training sample model that can be applied to more complicated background images, R. Li *et al.* [6] propose an image source identification method based on RSM. RSM obtains many new training sets via random sampling on the feature space of the training set. Training takes place on each new set separately, and then the results are combined to obtain the final identification result through majority vote. In the RSM method, assume that there are N images $\{I_i\}_{i=1}^n$ taken by C cameras $\{C_j\}_{j=1}^c$ in the database, and each camera took E_j images. First, build a feature subspace $T = [v_1, \dots, v_d] \in R^{N^2 \times d}$ by solving the eigenvalues and eigenvectors of the covariance matrix with SPN information and PCA. Second, select $m(m < d)$

eigenvectors randomly constituting subspace R , repeating this process L times to generate L subspaces R^l . SPN signal can be represented as: $y^l = R^{lT} x, l = 1, 2, \dots, L$. The reference SPN of cameras C_j obtained by averaging all training SPN belongs to this camera in the subspace R^l . Then calculate the correlation coefficient ρ between them. According to the relationship of ρ and threshold t , camera source identification problems can be regarded as a bidirectional hypothesis. If $\rho < t$, the query image is considered to have been taken by cameras C_j ; otherwise, the query image is considered to have been taken by other cameras. Finally, make the most of the L results as the final result.

Recently, deep learning has shown a quite remarkable performance in several computer vision tasks, such as image classification, object detection or image recognition. Unlike previous works focus on feature extraction, deep learning provides the unique ability to extract and learn features automatically from given data. V. U. Sameer *et.al* [11] put forward a novel two-level classification system based convolutional neural networks (CNN) model. At level one, the proposed system distinguishes between authentic and counter-forensically modified images, then at level two, the counter-forensic images are further classified according to some major classes of source anonymization attacks. The experimental results of identifying the device manufacturer prove that the maximum classification accuracy achieves 85.7%. D. Freire-Obregon *et.al* [12] describe a CNN architecture which is able to infer the noise pattern of mobile camera sensors. They conduct a set of experiments to validate the effectiveness of the proposed CNN model. The experimental results show that the identification accuracy is as high as 98.1% at model level, and the overall accuracy on sensor level is 91.1%. P. Yang *et.al* [13] propose a content-adaptive fusion network to identify the source camera of the small-size images, which is built by paralleling three adaptive-content convolutional neural networks to capture more comprehensive information. The experimental results demonstrate that the proposed algorithm achieves 94.17% for camera brand identification, 84.7% for model identification, and 70.19% for device identification.

To further improve identification accuracy, we want to analyze image complexity. In image processing, the complexity can be considered as the difficulty of extracting a feature in an image. Each image has many features, and thus the image complexity can be evaluated from multiple angles. Compared with other features, texture feature is able to balance the relationship between whole image and pixels and hence is more relevant in describing the complexity of an image. At the same time, the Gray Level Co-occurrence Matrix (GLCM) is widely used to analyze the texture features by calculating image statistics such as energy, entropy, and correlation. In GLCM, R. Haralick *et.al* [14] define 14 characteristic parameters to comprehensively analyze the aspect of texture. Commonly used parameters include the following: 1) Energy describes the uniformity coefficient of gray distribution and the crudeness or fineness degree of texture. The texture is more coarse and simple when the energy value is larger. 2) Contrast shows the sharpness of image and the depth degree of texture. The greater the contrast, the deeper the texture groove is, and the faster the brightness changes. 3) Entropy expresses the information content and texture complexity in the image. The image has fewer textures and lower complexity if the entropy is smaller. 4) Homogeneity means the local variation of the image texture. The larger the homogeneity, the less the local texture changes. 5) Correlation measures the correlation of local grayscale in an image. The image complexity decreases as the correlation value increases.

3. Proposed Scheme

Some areas in an image may contain much content, whereas other areas do not. As show in **Fig. 1**, the patch located at the bottom right corner of the image contains the building contour so that the extracted SPN must contain the information of the building. Although RSM is adopted, RSM still cannot totally reduce the effect of image content on SPN. The sky in the upper left corner of the image does not contain any image scene in which the extracted SPN is closer to pure SPN. So, we want to choose the sample area through some technical means to extract purer SPN rather than directly cut out the patch from the middle of the image, which further improves the identification accuracy.

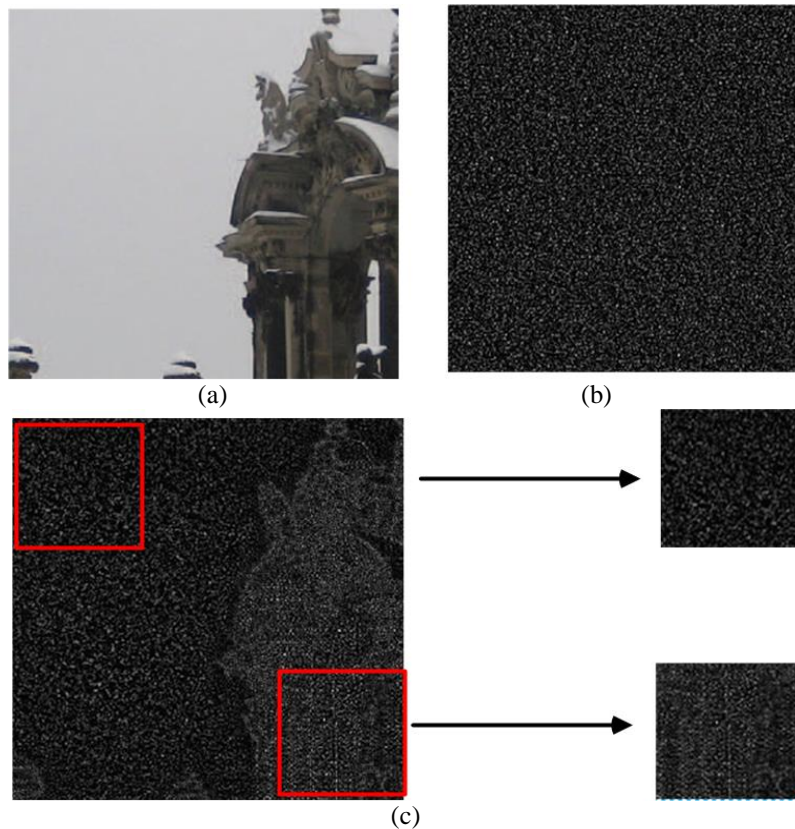


Fig. 1. (a) and (b) show the image and its pure SPN; (c) shows the extracted SPN from different areas, which make its purity different.

In GLCM, correlation measures the degree of similarity of GLCM elements in the row or column direction and describes the correlation of local grayscale in an image. When the GLCM elements are relatively uniform, the correlation value is larger, illustrating the greater degree of similarity of rows or columns and smaller image complexity.

$$COV = \sum_{i,j} \frac{(i - \mu_i)(j - \mu_j)G(i,j)}{\sigma_i \sigma_j} \quad (1)$$

where i, j represent the row and column, respectively, of GLCM G ; μ represents the normalized mean of one row or column, and σ denotes the matrix's mean squared error.

Ideally, the training images are supposed to be low change images, such as pure sky scenes, but the images adopted in the experiment do not conform to the requirements. According to the habit of taking photos, the scene that we want to record is typically in the middle position of an image. A patch directly cut out from the middle part of an image may contain more details, which will influence the identification accuracy. Thus, we want to choose an area with as little scene content as possible to extract a relatively pure SPN. In the present study, to reduce the computational cost, we only select the correlation in the GLCM to evaluate the image area complexity. Before extracting the SPN, we first partition each image in the dataset into many patches and calculate their correlation. Second, we select the patch with the largest correlation, namely the least complexity, to extract a relatively pure SPN. Finally, we go ahead with RSM, and in this way, we can obtain a better identification accuracy. An overview of the proposed algorithm is presented in [Alg.1](#).

Alg.1 sample selection method for image source identification

Input:

An image database $\{I_i\}_{i=1}^n$ taken by cameras $\{C_j\}_{j=1}^c$, E_j images for each camera.

A query image I_q .

Offline:

1: For $\forall I_i$, partition it into $p \times q$ patches with $N \times N$ size, analyze the image texture features, then select a patch with less complexity to extract a more reliable SPN x .

2: Build a feature subspace $T = [v_1, \dots, v_d] \in R^{N^2 \times d}$ by solving the covariance matrix S and PCA.

3: Select $m(m < d)$ eigenvectors randomly constituting subspace R , repeating L times, generate L subspaces R^l . SPN x can be represented as follows: $y^l = R^{lT} x, l = 1, 2, \dots, L$.

The reference SPN of camera C_j :

$$y_j^l = \frac{\sum_{i=1}^{E_j} y_i^l}{E_j}, \quad j = 1, 2, \dots, c$$

Online:

1: The SPN x of query image: $y_q^l = R^{lT} x, l = 1, 2, \dots, L$

2: Calculate the correlation coefficient: $\rho = \text{cov}(y_q^l, y_j^l) / (\sqrt{D(y_q^l)} \cdot \sqrt{D(y_j^l)})$

For a threshold t , if $\rho < t$, the query image is considered to have been taken by cameras C_j ; otherwise, the query image is considered to have been taken by other cameras. Make the most of the L results as the final result.

We need to cut a patch of size $N \times N$ to represent the entire image, taking computational expense into account. Because image resolutions are different, a patch of a size smaller than $N \times N$ will be filled with blanks during calculation. To avoid influencing the calculation result, we partition the image into $p \times q$ patches (p, q are integers) from the top left corner for each image; namely, each image can obtain a correlation matrix of size $p \times q$. For example, when $p = q = 4$, the image is cut into 4×4 patches, and we obtain a correlation matrix recording the patches correlation, as shown in [Fig. 2](#). According to the nature of the correlation, their values

are inversely proportional to complexity; that is, the greater the value, the smaller the complexity. Each image in the database repeats the calculation process above and sums up to a correlation matrix of the images set. Select the patch that has the largest correlation, namely, the smallest complexity, as the sample area to extract the SPN. The selected patch is the smoothest area in the dataset that contains less image content details and a relatively pure extracted SPN. Then combine this process with RSM, and the entire process is called the sample selection method (SSM).

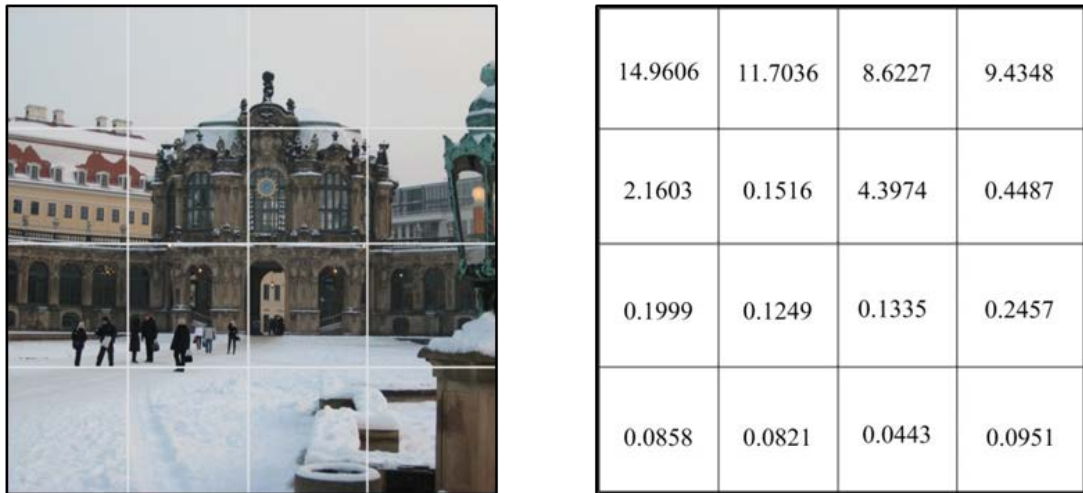


Fig. 2. The correlation of different patches in an image.
The patch that has the largest correlation has the least complexity.

4. Experimental Results and Analysis

4.1. Experimental setup

In order to validate the proposed SSM algorithm, we conduct a set of experiments on the Dresden database [15] that provide more than 16000 images took by 74 image devices. In this paper, we choose 10 camera devices and the list of camera devices are given in Table 1. There are 4 camera brands, each with two or three cameras individuals. Each individual camera is responsible for 120 images, with 50 images as the training images and the remaining as the test images. Repeat the experiment using the Lukas method, Lukas+PCA method, Lukas+RSM method and Lukas+SSM method and compare their average identification accuracy. Besides, some CNN models have achieved good experimental results for the image source identification task. In order to better evaluate the effectiveness of the proposed method, we compare the device-level average accuracy with the deep learning models mentioned in [11] - [13].

4.2. Performance evaluation

A. Lukas method

The Lukas method of image source identification based on pattern noise is calculating the correlation coefficient between the query and reference SPN. Judging the query image whether from one of the cameras according to the value of correlation coefficient. The experimental result has shown in Table 2.

Table 1. List of cameras used in experiments

Cameras	Resolutions	Alias
Canon_Ixus70_0	3072×2304	C1
Canon_Ixus70_1	3072×2304	C2
Canon_Ixus70_2	3072×2304	C3
Nikon_CoolPixS710_0	4352×3264	N1
Nikon_CoolPixS710_1	4352×3264	N2
Samsung_L74wide_0	3072×2304	S1
Samsung_L74wide_1	3072×2304	S2
Samsung_L74wide_2	3072×2304	S3
Olympus_mju_1050SW_0	3648×2734	O1
Olympus_mju_1050SW_1	3648×2734	O2

Table 2. Accuracy of the Lukas method(%)

	C1	C2	C3	N1	N2	S1	S2	S3	O1	O2
C1	98.6	0	0	0	1.4	0	0	0	0	0
C2	0	98.6	0	0	0	1.4	0	0	0	0
C3	0	0	100	0	0	0	0	0	0	0
N1	1.4	4.3	4.3	65.7	10	1.4	4.3	1.4	4.3	2.9
N2	0	0	2.9	4.3	92.8	0	0	0	0	0
S1	2.9	0	0	0	0	91.4	5.7	0	0	0
S2	2.9	1.4	2.9	2.9	1.4	0	77	2.9	4.3	4.3
S3	1.4	0	2.9	2.9	2.9	1.4	0	88.5	0	0
O1	0	1.4	1.4	2.9	0	1.4	2.9	0	77.1	12.9
O2	1.4	0	1.4	0	0	1.4	2.9	1.4	8.6	82.9

From the experimental result, we can obtain the average identification accuracy is 87.3% by averaging these numbers. In addition, different individual cameras of same camera model are more likely to lead miscalculation. However, there are not mutual misunderstanding among cameras C1, C2 and C3. It is mainly because the reference SPNs are purer.

B. Lukas+PCA method

PCA retains the feature vectors with greater discriminative, thus reduces the dimension of calculation under the premise of representing original data as good as possible. Once selecting an appropriate proportion of principal component, PCA can improve the identification accuracy to a certain extent.

First of all, we analyze the influence of cumulative contribution rate $G(m)$ on identification accuracy. The identification accuracy with the change of $G(m)$ is shown in **Fig.**

3. We can find the accuracy increases as $G(m)$ increases and it is lower than Lukas method when $G(m) < 99\%$, because some useful information is considered redundant information and deleted. When $G(m) = 99\%$, the accuracy is slightly higher than the Lukas method. At this point, the dimension of SPN decreases from 500 to 413. The experimental result has shown in **Table 3**.

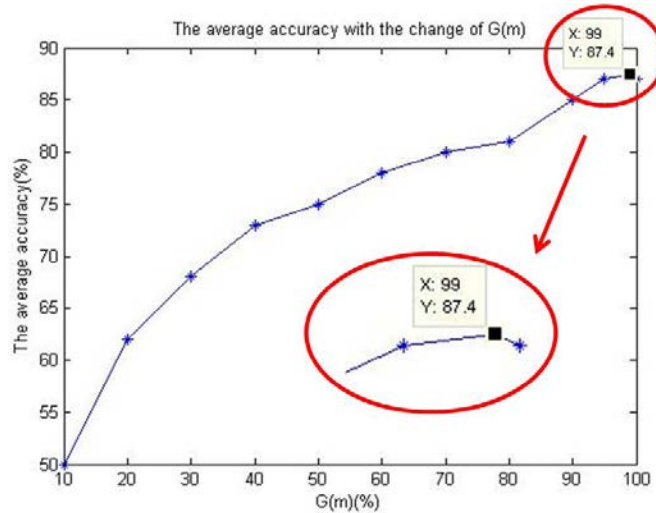


Fig. 3. The identification accuracy with the change of $G(m)$

Table 3. Accuracy of the Lukas+PCA method(%)

	C1	C2	C3	N1	N2	S1	S2	S3	O1	O2
C1	97.2	0	1.4	0	1.4	0	0	0	0	0
C2	1.4	98.6	0	0	0	0	0	0	0	0
C3	0	0	100	0	0	0	0	0	0	0
N1	2.9	4.3	4.3	65.6	11.4	1.4	2.9	1.4	2.9	2.9
N2	0	0	2.9	4.3	92.8	0	0	0	0	0
S1	2.9	0	0	0	0	92.8	4.3	0	0	0
S2	2.9	1.4	2.9	2.9	1.4	0	77	2.9	4.3	4.3
S3	1.4	0	1.4	2.9	2.9	1.4	0	90	0	0
O1	0	2.9	1.4	2.9	0	1.4	2.9	0	75.6	12.9
O2	0	0	1.4	1.4	0	1.4	2.9	0	8.6	84.3

The average identification accuracy is 87.4% obtained from **Table 3**. Compared with the Lukas method, it increases 0.1% in the case of decreasing SPN dimension. Therefore, PCA can improve identification accuracy through removing noise and redundancy which are useless for identification when choose an appropriate cumulative contribution rate $G(m)$.

C. Lukas+RSM method

Lukas+RSM method can further suppress image scene content effect on SPN. Two experiments respectively to observe the influence of parameters L and M/d on accuracy. First, fix L and adjust M/d, observing the sensitivity of the parameter M/d. Second, choose and fix a proper M/d and adjust L. The result is shown in Fig. 4. We find that the performance is not sensitive to the parameters L and M/d. The best performance appears when M/d = 0.3 and L = 400 and there is a tradeoff between the performance and the computational complexity. The result of identification is shown in Table 4.

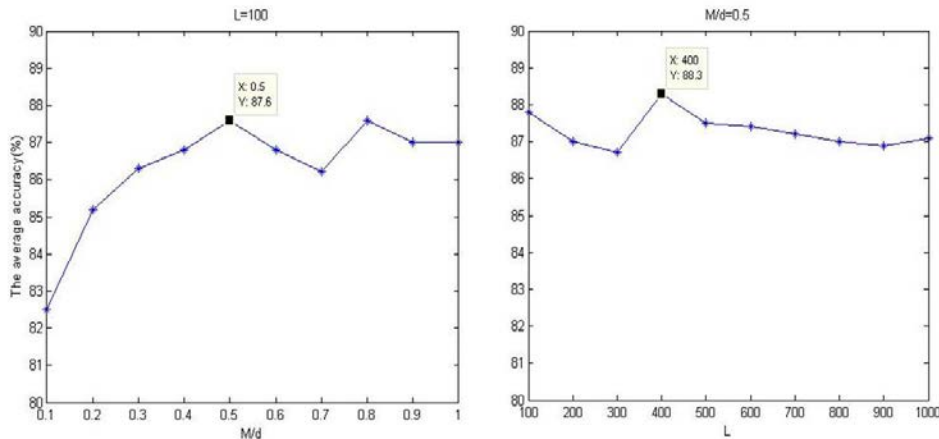


Fig. 4. The effects of parameters M and L/d

Table 4. Accuracy of Lukas+RSM method when M/d=0.5, L=400(%)

	C1	C2	C3	N1	N2	S1	S2	S3	O1	O2
C1	95.7	0	2.9	0	0	0	0	0	1.4	0
C2	1.4	95.8	1.4	0	0	0	0	1.4	0	0
C3	0	0	98.6	1.4	0	0	0	0	0	0
N1	4.3	0	1.4	81.4	2.9	2.9	0	1.4	4.3	1.4
N2	5.7	0	0	1.4	88.7	0	1.4	1.4	1.4	0
S1	4.3	4.3	1.4	0	1.4	84.3	0	0	1.4	2.9
S2	2.9	0	2.9	2.9	0	1.4	88.5	1.4	0	0
S3	0	0	0	1.4	0	0	0	95.7	0	2.9
O1	2.9	1.4	0	0	0	0	0	1.4	77.2	17.1
O2	1.4	0	0	0	0	0	1.4	0	20	77.2

The average identification accuracy of Lukas+RSM method is 88.3%, increases 0.9% compared with the Lukas+PCA method. It shows that RSM can effectively inhibit the influence of scene details to some extent.

D. Lukas+SSM method

In the Lukas+RSM method, we cut out a pixel block of size 256×256 from the central part of each image to extract the pattern noise in the experiment. In our proposed method, at the beginning of the identification process, we evaluate the complexity of image regions to extract more reliable pattern noise. Each image is cut into 2048×2048 from the top left corner, so every image can yield 8×8 patches whose size is 256×256 ; namely, we obtain 8×8 correlation matrixes. The image grayscale is compressed to 16 for the sake of simplifying the computation of GLCM. The process above is repeated for a total of 1200 images used in the experiments, which yields a correlation matrix of image set. The patch correlation is shown in [Table 5](#).

Table 5. The patch correlation in dataset (10^4)

1.3610	1.5925	1.4586	1.2352	1.4163	1.2155	1.5770	1.3235
1.4200	1.2593	0.9244	1.2302	0.9442	1.2868	1.5716	1.3474
1.0984	0.8087	0.7612	1.0199	1.2054	1.0570	1.2178	1.1123
1.1353	0.6064	0.5761	0.6027	0.8489	0.7015	0.5064	0.7193
0.5969	0.4425	0.3381	0.6384	0.4943	0.3305	0.2352	0.7417
0.4119	0.4034	0.4896	0.4890	0.2098	0.1629	0.2229	0.2415
0.4419	0.5472	0.7511	0.5914	0.3907	0.3329	0.3395	0.3156
0.6491	0.5252	0.7422	0.6516	0.7076	0.5305	0.4543	0.4978

From [Table 5](#), the patch located at the second column of the first line has the smallest complexity. Therefore, we extract the pattern noise from this patch to observe the identification accuracy of the sample selection method. Because the experimental area has changed, we need to select the value of the parameter L and M/d. The same as the previous steps and the result is shown in [Fig. 5](#). We find that the performance is not sensitive to the parameters L and M/d. The best performance appears when $M/d = 0.3$ and $L = 400$ and there is a tradeoff between the performance and the computational complexity. Thus, we set experimental parameters $M/d = 0.3$ and $L = 400$ because these values generate the best result. The specific identification accuracy of each camera is calculated to a decimal fraction and shown in [Table 6](#).

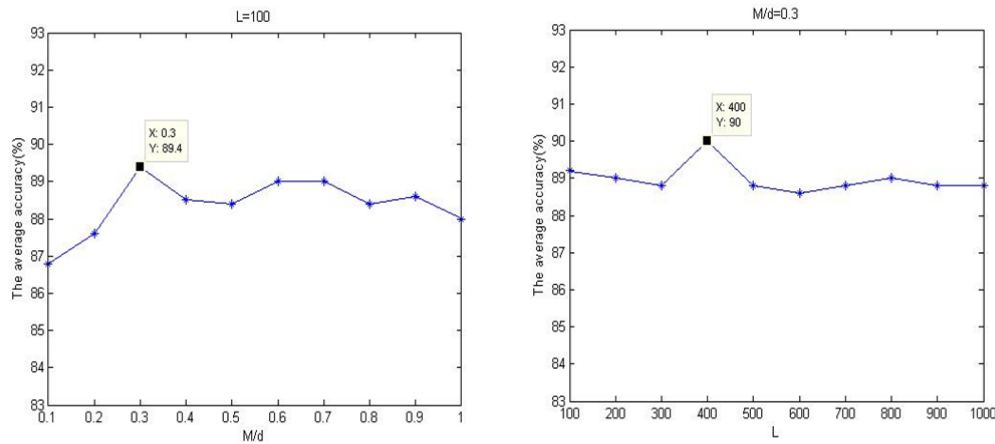


Fig. 5. The effects of parameters M and L/d

Table 6. Sample selection method accuracy when M/d=0.3, L=400(%)

	C1	C2	C3	N1	N2	S1	S2	S3	O1	O2
C1	97.2	1.4	1.4	0	0	0	0	0	0	0
C2	1.4	95.8	1.4	0	0	0	0	0	0	1.4
C3	0	0	98.6	1.4	0	0	0	0	0	0
N1	2.9	0	1.4	84.2	2.9	2.9	0	1.4	1.4	2.9
N2	5.7	0	0	2.9	88.6	0	1.4	0	1.4	0
S1	2.9	2.9	4.3	0	0	87.1	0	0	1.4	1.4
S2	2.9	0	2.9	1.4	0	1.4	88.6	1.4	0	1.4
S3	0	0	0	0	0	0	0	95.7	0	4.3
O1	2.9	1.4	1.4	0	0	0	0	1.4	80	12.9
O2	1.4	0	0	0	0	0	0	0	14.3	84.3

Table 6 indicates the identification accuracy of each camera. The numbers on the main diagonal denote the probability of correct judgment, and we can obtain an average identification accuracy of Lukas+SSM of 90% by averaging these numbers.

Comparing the experimental data, it can be inferred that the performance is quite good in the case of identifying the source device of the image. However, it may slightly degrade when there are multiple cameras belonging to the same model. This is due to the strong feature similarity between same camera models. For instance, it is more complicated to distinguish images taken from O1 and O2 than distinguishing images taken from C1 and S3.

The average accuracy of 10 cameras, camera N1 and O1 in the four methods is shown in Fig. 6. The identification accuracy of camera N1 and O1 in Lukas+SSM are significantly improved compared with other methods. The original identification accuracy of the other cameras is great; although there is no obvious identification accuracy improvement in Lukas+SSM, this method still maintains the original high accuracy, which shows that our proposed SSM has a certain robustness.

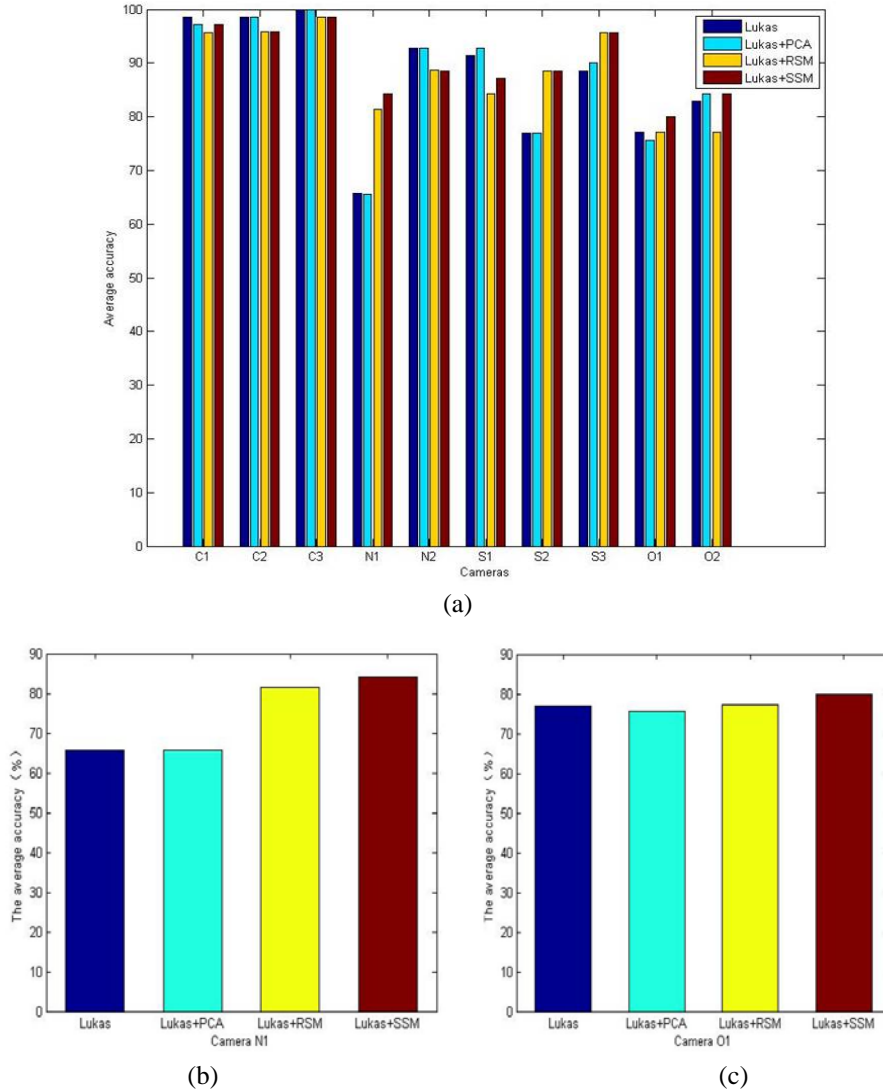


Fig. 6. (a): The average accuracy of 10 cameras in these four methods.
(b) and (c): The average accuracy of camera N1 and O1

The top half of **Table 7** reports a comparison with the average identification accuracy of four traditional methods. Note that the Lukas+PCA method retains 99% of the information and the Lukas+RSM method selects experimental parameters $M/d = 0.5$, $L = 400$, which shows that extracting pattern noise from smaller complexity patch can effectively improve the identification accuracy. It can be observed that the proposed method, Lukas+SSM, achieves encouraging identification accuracy in all traditional methods. Although the performance increase is not large, the simplicity of the proposed approach leaves room for future work.

E. Compare with deep learning models

In order to better assess the performance of the proposed method, we also compare the average accuracy with the deep learning models mentioned in [11] - [13]. The device-level experimental results from the corresponding articles are marked as ⁺, and shown in the lower part of **Table 7**.

Results show the CNN model proposed by D. Freire-Obregon et.al achieves an average accuracy rate of 91.1%, which is better than other two deep learning models for camera source identification task, even 1.1% better than the Lukas+SSM method. However, compared with the SSM method, this method is more complex. In order to ensure a CNN model gets a good performance, network structure must be well-designed and a lot of parameters, such as weights, learning rate etc. , must be determined through an iterative training process. The training process requires a lot of well-marked data, which will takes a lot of time and manpower. More importantly, When the experimental data changes, the network parameters need to be re-adjusted by training process. But the proposed SSM method does not need so much tagging data and repeated training, still able to reach a good identification results.

Table 7. Comparison results

Schemes		Average accuracy
Traditional methods	Lukas	87.3%
	Lukas+PCA	87.4%
	Lukas+RSM	88.3%
	Lukas+SSM	90%
Deep learning models	P. Yang et.al [13]	70.19% ⁺
	V. U. Sameer et.al [11]	85.7% ⁺
	D. Freire-Obregon et.al [12]	91.1% ⁺

5. Conclusion

The sensor pattern noise is an inherent fingerprint of image equipment, which can effectively identify the source of digital images. In a previous study, a random subspace method based on the sensor pattern noise achieved a good result but was still affected by image details. To further reduce the influence of details, we proposed the sample selection method. By selecting a patch with less complexity, we can extract purer pattern noise and further optimize the identification performance. We conduct experiments on four traditional methods and contrast the device-level identification accuracy with some state-of-the-art deep learning methods. The experimental results show that our proposed sample selection can further improve the identification accuracy compared to other related traditional methods. At the same time, the proposed method is less complex and close to the most advanced performance compared with the latest deep learning models.

References

- [1] K. S. Choi, E. Y. Lam, and K. K. Wong, "Automatic source camera identification using the intrinsic lens radial distortion," *Optics Express*, vol. 14, no. 24, pp.11551-11565,2006. [Article \(CrossRef Link\)](#)
- [2] John S. Ho, Oscar C. Au, Jiantao Zhou, and Yuanfang Guo. "Inter-channel demosaicking traces for digital image forensics," in *Proc. of IEEE International Conference on Multimedia and Expo(ICME)*, pp.1475-1480, July 19-23, 2010. [Article \(CrossRef Link\)](#)

- [3] Q. Liu, X. Li, and L. Chen, "Identification of smartphone-image source and manipulation," in *Proc. of International Conference on Industrial Engineering and Other Applications of Applied Intelligent Systems: Advanced Research in Applied Artificial Intelligence(IEA/AIE)*, pp.262-271, June 9-12, 2012. [Article \(CrossRef Link\)](#)
- [4] J. Lukas, J. Fridrich, and M. Goljan, "Digital camera identification from sensor pattern noise," *IEEE Transactions on Information Forensics & Security*, vol. 1, no.2, pp. 205-214, June, 2006. [Article \(CrossRef Link\)](#)
- [5] R. Li, C. T. Li, and Y. Guan, "A compact representation of sensor fingerprint for camera identification and fingerprint matching," in *Proc. of IEEE International Conference on Acoustics, Speech and Signal Processing(ICASSP)*, pp. 1777-1781, April 19-24, 2015. [Article \(CrossRef Link\)](#)
- [6] R. Li, C. Kotropoulos, C. T. Li, and Y. Guan, "Random subspace method for source camera identification," in *Proc. of IEEE International Workshop on Machine Learning for Signal Processing (MLSP)*, pp. 1-5, September 17-20, 2015. [Article \(CrossRef Link\)](#)
- [7] Z. Li, J. Liu, Y. Yang, and et al, "Clustering-guided sparse structural learning for unsupervised feature selection," *IEEE Transactions on Knowledge & Data Engineering*, vol.26, no.9, pp. 2138-2150, September, 2014. [Article \(CrossRef Link\)](#)
- [8] Z. Li and J. Tang, "Unsupervised feature selection via nonnegative spectral analysis and redundancy control," *IEEE Transactions on Image Processing*, vol.24, no.12, pp. 5343-5355, December, 2015. [Article \(CrossRef Link\)](#)
- [9] Z. Li, J. Liu, J. Tang, and H. Lu, "Robust structured subspace learning for data representation," *IEEE Transactions on Pattern Analysis & Machine Intelligence*, vol.37, no.10, pp. 2085-2098, October, 2015. [Article \(CrossRef Link\)](#)
- [10] L. Zheng, R. Lukac, X. Wu and D. Zhang, "PCA-based spatially adaptive denoising of CFA images for single-sensor digital cameras," *IEEE Transactions on Image Processing*, vol.18. no.4, pp.797-812, April, 2009. [Article \(CrossRef Link\)](#)
- [11] V.U. Sameer, R. Naskar, N. Musthyala, and K. Kokkalla, "Deep learning based counter-forensic image classification for camera model identification," *Digital Forensics and Watermarking*, pp.52-64, August 23-25, 2017. [Article \(CrossRef Link\)](#)
- [12] D. Freire-Obregón, F. Narducci, S. Barra, and M. Castrillón-Santana, "Deep learning for source camera identification on mobile devices," arXiv:1710.01257. [Article \(CrossRef Link\)](#)
- [13] P. Yang, W. Zhao, R. Ni, and Y. Zhao, "Source camera identification based on content-adaptive fusion network," arXiv:1703.04856. [Article \(CrossRef Link\)](#)
- [14] R. M. Haralick, K. Shanmugam, and I. Dinstein, "Textural Features for Image Classification," *IEEE Transactions on Systems Man & Cybernetics*, vol.3, no.6, pp.610-621, November, 1973. [Article \(CrossRef Link\)](#)
- [15] T.Gloe and R. Böhme, "The 'Dresden Image Database' for benchmarking digital image forensics," in *Proc. of ACM Symposium on Applied Computing (SAC)*, pp.1584-1590, March 22-26, 2010. [Article \(CrossRef Link\)](#)



Zhihui Wang received the B.S. degree in software engineering in 2004 from the North Eastern University, Shenyang, China. She received her M.S. degree in software engineering in 2007 and the Ph.D degree in software and theory of computer in 2010, both from the Dalian University of Technology, Dalian, China. Since November 2011, she has been a visiting scholar of University of Washington. Her current research interests include information hiding and image compression.



Hong Wang graduated in Electronic and Information Engineering in 2016 from Dalian University of Technology. She is a graduate student at the School of Software Technology in Dalian University of Technology. Her current research interests in image processing and object retrieval.



Haojie Li is a Professor in the School of Software, Dalian University of Technology. His research interests include social media computing and multimedia information retrieval. He has co-authored over 50 journal and conference papers in these areas, including IEEE TCSVT, TMM, TIP, ACM Multimedia, ACM ICMR, etc. Dr. Li received the B.E. and the Ph. D. degrees from Nankai University, Tianjin and the Institute of Computing Technology, Chinese Academy of Sciences, Beijing, in 1996 and 2007 respectively. From 2007 to 2009, he was a Research Fellow in the School of Computing, National University of Singapore. He is a member of IEEE and ACM.